Luminescence Quenching in Polymer/Filler Nanocomposite Films Used in Oxygen Sensors

Xin Lu and Mitchell A. Winnik*

Department of Chemistry, University of Toronto, 80 St. George Street, Toronto, Ontario M5S 3H6, Canada

Received February 5, 2001. Revised Manuscript Received July 24, 2001

Luminescent oxygen sensors are devices in which the active element involves a luminescent dye in a polymer film. Oxygen partitions into the polymer from an adjacent gas or liquid phase and quenches the dye luminescence to an extent that depends on the amount of oxygen present in the film. When the dyes are dissolved in or attached to the molecules of a pure polymer film, the quenching kinetics can be described completely in terms of parameters that can be determined independently: the excited-state lifetime of the dye and the permeability (P_{O_2}) and diffusion coefficient (D_{O_2}) of oxygen in the polymer. In many sensors, nanometer-sized inorganic particles are often added to the active matrix. These particles are added either as carriers for the dye molecules or to reinforce the polymer film. The presence of these particles in the polymer complicates the quenching kinetics, because both the dyes and the oxygen molecules partition between the polymer matrix and the particle surfaces. The purpose of this article is to review the factors that operate to affect quenching kinetics in particle-filled polymer films. We provide a brief review of polymer composite systems used in sensors and a more detailed review of the factors that affect quenching kinetics in these systems. We end with a description of more sophisticated models that have been employed to analyze oxygen quenching of dyes adsorbed on the surface of inorganic particles in the hopes that similar models might be developed in the future to describe oxygen quenching in polymer composite films.

Introduction

Polymer films containing luminescent dyes are widely used in oxygen sensors.[1−8] These applications take advantage of the high efficiency with which oxygen quenches the excited state of the dyes. The polymer matrix serves as a matrix for supporting the dye and also as a medium for oxygen transport from the surroundings. To maximize the effectiveness of the sensor, one often chooses dyes with long unquenched excited-state lifetimes τ^o, polymers with high oxygen permeabilities P_{O_2}, and polymer−dye combinations in which the dye dissolves in the polymer. At the same time, one should also note that there is always a tradeoff between the sensitivity of sensors to the oxygen concentration and the signal-to-noise (S/N) limitations because the luminescence intensity of the sensors is rather low when the luminescence quenching is very strong.[5,8−10] Luminescent transition metal complexes, especially those containing platinum or ruthenium, have shown considerable promise in oxygen-sensing applications. Many of these dyes have the desirable features of long lifetimes; convenient excitation and emission wavelengths; large Stokes shifts; reasonable luminescence quantum yields; and relatively good thermal, chemical, and photochemical stability. Linear poly(dimethyl siloxane) (PDMS) and many silicone resins have high permeabilities to oxygen.[5] Most of the papers appearing in the analytical chemistry literature employ cross-linked silicone resins as the sensor matrix. The surrounding medium can be a liquid such as blood or groundwater or a gas such as air.[1,6,7] The specific application in which the sensor is painted over a surface to serve as a two-dimensional air pressure profile sensor for objects exposed to wind flow is referred to as "phosphorescence barometry", and the engineers refer to the coating as "pressure-sensitive paint" (PSP).[2−4,8]

This review is concerned with the addition of inorganic particles of nanometer size to polymer matrixes to enhance the performance of sensors. These particles can serve three separate functions. First, in cases where the dye is poorly soluble in the polymer itself, the inorganic particles serve as carriers for the dye molecules, which are thought to be bound to the particle surface or trapped inside the porous structure. Second, the particles are added as "fillers" to reinforce the polymer film, improving its mechanical properties. Finally, when the volume fraction of filler is so large that the polymer phase is no longer continuous, voids are created. These voids enhance the air-exposed surface area of the sensor and change its optical properties.

The presence of the inorganic particles in the hybrid structure complicates enormously our ability to understand how the fundamental mechanisms of oxygen transport and luminescence quenching affect sensor performance. From the perspective of the dye, a certain, often large, fraction of the dye is adsorbed onto the particle surface. On the surface, it can experience a range of environments, each with its own characteristic lifetime. The enhanced dye concentration at the particle surface can promote dye aggregation. Dye aggregates

10.1021/cm011029k CCC: $20.00
Published on Web 09/20/2001

often have different excited-state lifetimes, different absorption and emission spectra, and different sensitivities to oxygen quenching. In addition, some dye aggregates are nonemissive. From the polymer's perspective, the particles increase the modulus of the polymer and reduce the tendency of two slabs of polymer to adhere (i.e., the filler increases the block resistance of the polymer).[11] These are the major reasons for adding the filler to the matrix. The nature of the polymer−filler interaction depends sensitively on the nature of the inorganic particle surface as well as the state of particle aggregation in the system. In the case of silica, the method of preparation (fumed silica, sol−gel silica), the method of surface treatment, and the method of compounding the silica into the polymer have large effects on the properties of the composite matrix.

From the perspective of the oxygen molecules, the filler has two types of impact. First, oxygen molecules can adsorb onto the particle surface. This increases the overall content of oxygen in the system and makes it much more difficult to describe the distribution of oxygen in the system. Second, the filler particles can perturb the diffusion of oxygen in the matrix. By decreasing the mobility of polymer segments near their surfaces, the inorganic particles can reduce the diffusion rate of oxygen in their vicinity. By acting as obstacles, the inorganic particles can increase the tortuosity of the oxygen diffusion path. By adsorbing oxygen molecules from the matrix, the particles can either retard the oxygen diffusion rate by acting as local oxygen reservoirs or enhance the diffusion rate through rapid oxygen diffusion along the particle surface. In many of the papers we cite, the nature of the particle surface is largely unknown. Nevertheless, one can imagine that the detailed nature of the surface plays an important role in determining the dye adsorption, the oxygen adsorption onto and diffusion along the surface, and the strength of particle interactions with the polymer matrix.

In this review, we focus on the effect of mineral fillers of nanometer dimensions on the performance of luminescent oxygen sensors based on polymers with high oxygen permeabilities. There is an extensive literature on fluorescence and phosphorescence quenching for dyes bound to the surface of silica and other minerals. We cite selective papers from this field to help elucidate how the particle surfaces affect oxygen quenching of surface-bound dyes. There is an even more extensive literature on inorganic particles as mineral fillers for polymers.[11−14] This is a topic beyond the scope of the current review. Although our focus is on nanocomposites, some of the papers we cite employ micrometer-sized mineral particles. Here, unless particle size has a specific impact on the performance of the sensor, we will mention particle size only as a detail of the experiment.

In the following sections, we first present an overview of the use of polymer−mineral nanocomposites as luminescent oxygen sensors, which begins with a brief introduction to oxygen quenching kinetics for dyes dissolved in polymer matrixes. The second section focuses on luminescence experiments to determine oxygen diffusion in polymers and how this diffusion is affected by the presence of inorganic particles. The third section discusses how these particles can influence the solubility of oxygen in the composite. In the fourth section, we examine luminescence quenching for the specific case of dyes bound to the surface of silica particles, where the quenching kinetics have been studied in some detail. We close with a brief summary.

We end this introduction with a comment on terminology. In industry, the inorganic mineral component added as small particles to a polymer matrix is commonly referred to as a "filler". In the coatings industry, these fillers are commonly added as light-scattering centers, i.e., as opacifying agents, and are referred to as "pigments." We will refer to the mineral additive as the filler when we speak in general terms about this component of a polymer−inorganic composite. We will sometimes use the term inorganic nanoparticles when we wish to emphasize that the filler consists of nanometer-sized spheres with a narrow size distribution.

Overview

Quenching Kinetics. Luminescent oxygen sensors depend on the diffusion-controlled quenching (or dynamic quenching) of dye fluorescence or phosphorescence by oxygen.[15,16] Dynamic quenching is described by the Stern−Volmer equation

$$\frac{I^o}{I} = \frac{\tau^o}{\tau} = 1 + k_q \tau^o [O_2] \tag{1}$$

where I is the intensity and τ is the lifetime of the dye and I^o and τ^o are the corresponding values in the absence of oxygen, k_q is the quenching rate constant, and $[O_2]$ is the molar concentration of oxygen. When the polymer film is present in an air environment and the gas pressure is not very high, the equilibrium oxygen concentration in the polymer film is proportional to the oxygen partial pressure (p_{O_2}) just above the film

$$[O_2] = S_{O_2} p_{O_2} \tag{2}$$

where the proportionality constant, S_{O_2}, is the oxygen solubility defined by Henry's law.

The solubility of oxygen in most organic solvents and polymers at 1 atm air pressure is rather low, around $\sim 10^{-3}-10^{-2}$ M.[17] The rate constants for quenching of the excited states by the molecular oxygen in organic solvents are reported to be $\sim 10^9-10^{10}$ M^{-1} s^{-1}.[18] In solid polymer matrixes, the quenching rate constant is smaller [i.e., 1.7×10^8 M^{-1} s^{-1} for polystyrene and 4.6×10^7 M^{-1} s^{-1} for poly(ethyl methacrylate)].[19] Therefore, the product $k_q[O_2]$ is commonly less than 10^7 s^{-1}. Effective quenching can be observed only if the value of $1/\tau^o$ is comparable to or less than the value of $k_q[O_2]$. Unless the oxygen concentration and oxygen mobility in a polymer matrix are unusually large, luminescent dyes with short-lived electronically excited states (<0.1 μs) cannot be used for oxygen sensing applications.

For quenching influenced by diffusion, the quenching rate constant is related to the diffusion-controlled rate constant, k_{diff}, for complex formation between oxygen and the excited dye molecules by the expression

$$k_q = \alpha k_{diff} \tag{3}$$

where α represents the probability that a collision leads to quenching. Although α is expected to be unity for

quenching of singlet excited states,[20] several authors[21,22] have argued that α is at most $^1/_9$ for phosphorescence quenching by oxygen. The way in which spin statistics enter into triplet quenching is rather subtle, and many authors simply set α equal to unity in analyzing their data.[23] For example, in the theory of partially diffusion-controlled reactions,[24] α increases as the diffusion coefficient of quenchers decreases. In the Smoluchowski description of diffusion-controlled reactions,[25] k_{diff} depends on the sum of the diffusion coefficients of the dye and quencher. However, in the case of much faster oxygen diffusion, $D_{O_2} + D_{dye} \approx D_{O_2}$, and

$$k_{diff} = \frac{4\pi N_A \sigma}{1000} D_{O_2} \qquad (4)$$

where N_A is Avogadro's number and σ is the collision radius of the oxygen−dye complex. Upon substitution of eqs 2−4 into eq 1, one obtains

$$\frac{I^o}{I} = \frac{\tau^o}{\tau} = 1 + \frac{4}{1000}\pi\sigma\alpha N_A \tau^o (D_{O_2} S_{O_2}) p_{O_2} \qquad (5)$$

Equation 5 is the fundamental expression governing luminescence quenching by oxygen for systems in equilibrium with oxygen in the gas phase. The extent of quenching depends on the oxygen permeability, P_{O_2}, of the matrix, where P_{O_2} is defined as the product of D_{O_2} and S_{O_2}. For sensors employed to monitor the concentration of oxygen in liquids, the product $S_{O_2}p_{O_2}$ has to be replaced by the product of the partition coefficient for oxygen times the oxygen concentration in the liquid sampled.

The derivation of eq 5 assumes a homogeneous environment for the dye molecules and a uniform distribution of oxygen molecules in the polymer matrix. We emphasize this point because many sensor experiments employ dyes that exhibit nonexponential decay profiles, even in the absence of oxygen. In other systems, where the excited dye itself undergoes simple first-order decay in the absence of quencher, the decays become nonexponential in the presence of oxygen. Nonexponential decays in the absence of quencher point to a distribution of emitting species in the system. When the unquenched decay of the excited dye is exponential, deviations from simple pseudo-first-order kinetics in the presence of quencher are likely to be connected to spatial variations in quencher concentration, which do not equilibrate on the time scale defined by τ^o.[5]

From eq 5, we see that the sensitivity to oxygen of a given polymer−dye combination depends on the product of P_{O_2} and τ^o. For experiments intended to detect low concentrations or low partial pressures of oxygen, one would like the unquenched lifetime to be long (hundreds of nanoseconds to 100 μs), hence the use of phosphorescent dyes, because the triplet excited state has a longer lifetime than the singlet excited state.[1,5,7,8] In Figure 1, we present the structures of several dyes commonly used in sensor applications. It is also desirable for the permeability of the matrix to oxygen to be high, thus the use of silicone-based polymers. For sensor applications in which one attempts to detect small changes in oxygen concentration ($\Delta[O_2]$) or oxygen pressure (Δp_{O_2}), the choice is made differently. If the product $P_{O_2}\tau^o$ is too large at the mean pressure to be sampled (p_{mean}), then the luminescence intensity at this pressure (I_{mean}) will be too small to allow accurate measurements to be made. Under these circumstances, one should choose a dye−polymer combination with $I^o/I_{mean} = 2$, so that small changes in p_{O_2} in the vicinity of p_{mean} lie in the range of the maximum sensitivity to quenching.[5−10]

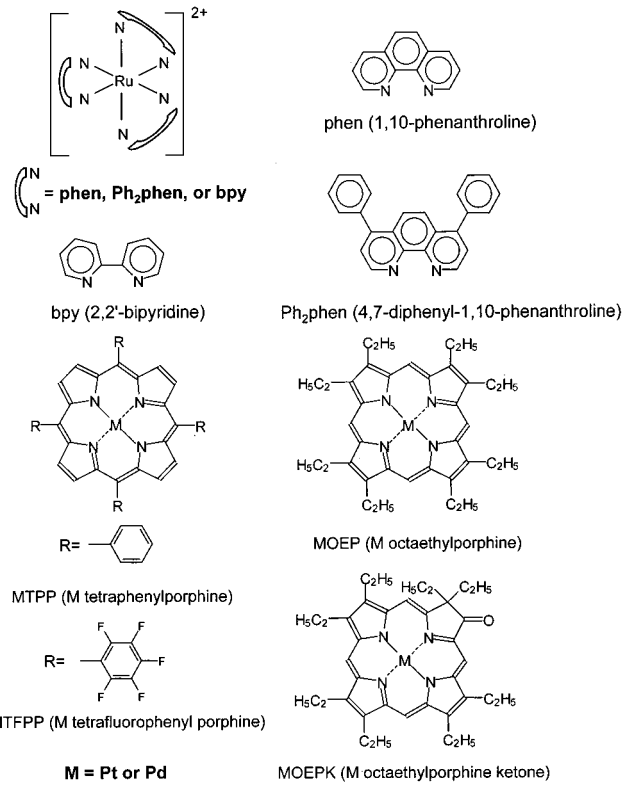

Figure 1. Representative probe molecules used for luminescent oxygen sensors.

For polymer scientists, eq 5 provides a useful way of obtaining values of P_{O_2} from luminescence quenching experiments carried out on polymers equilibrated with a series of oxygen partial pressures. The 1986 chapter by Guillet[26] is a very useful review of the early experiments used to obtain these values. To obtain individual values of D_{O_2} and S_{O_2}, one has to carry out time-scan experiments to monitor the diffusion of oxygen into or out of the polymer matrix. The data then have to be interpreted in a way that couples Fick's law of diffusion[27] to the details of the experiment in which luminescence is detected. Cox et al.[28−30] measured oxygen diffusion by fluorescence quenching in a silicone matrix containing 9,10-diphenylanthracene. The resin filled a tube exposed to oxygen at one end, and they monitored the fluorescence intensity as a function of time at a specific position along the tube. Ogilby and his group[31−33] used the direct phosphorescence of singlet oxygen to monitor the growth in concentration of oxygen in polymer films. The Winnik and Manners groups[34−38] have used time-scan experiments to measure the decay of luminescence intensity as oxygen diffuses into polymer films under constant illumination and the growth of intensity as oxygen diffuses out of the film. Their data were interpreted with the aid of theoretical expressions, derived by Mills and Chang[39] and by Yekta et al.,[21a] that couple Stern−Volmer quenching kinetics with Fick's laws of diffusion.

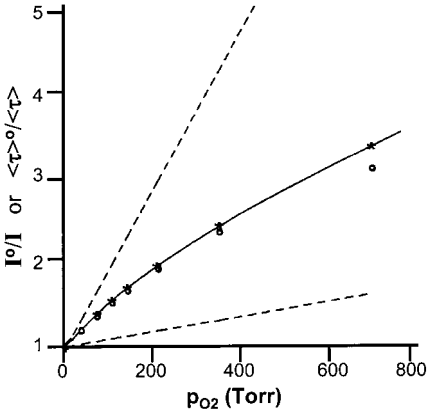

Figure 2. Stern−Volmer plots from ref 43 of intensity I^o/I (*) and lifetime $\langle\tau\rangle^o/\langle\tau\rangle$ (○) ratios versus p_{O_2} for $Ru(bpy)_3Cl_2$ adsorbed on silica gel. The continuous line represents the best fit to a two-site model (eq 23); and the dashed lines 1 and 2 represent the respective components in the model. $K_{SV1} = 9.2 \times 10^{-3}$ Torr^{-1}, $K_{SV2} = 0.9 \times 10^{-3}$ Torr^{-1}, $f_{01} = 0.66$, $f_{02} = 0.34$. Copyright 1995 Elsevier Science.

Sensors Containing Fillers. Many luminescent oxygen sensors are based on silicone resins. Silicone resins are oligomeric or low-molecular-weight polymers based on Si−O repeat units, commonly dimethyl siloxane units [$(CH_3)_2Si-O$], with pendant or terminal functional groups that allow the polymer to become cross-linked once it is applied to a substrate. Cross-linking converts the matrix into a single molecule of macroscopic dimensions. There are many different silicone resins, and commercial resins often have a proprietary structure.

From a historical perspective, the first dyes employed in luminescent oxygen sensors were ionic dyes based on ruthenium. Because these dyes were not very soluble in the nonpolar silicone resins, inorganic pigments were used as carrier vehicles for the dyes. In 1986, the Wolfbeis research group[40] reported an oxygen-sensing material prepared by treating porous silica particles (Lichrospher 300) with an aqueous solution of a ruthenium dye [tris(2,2′-bipyridyl)Ru(II) dichloride, $Ru(bpy)_3Cl_2$] and then dispersing the dry pigment in a silicone polymer. They used this material to fabricate an optical fiber oxygen sensor.[41] Both phosphorescence intensities[40] and decay profiles[42] were measured as functions of the oxygen pressure. Nonlinear Stern−Volmer plots were obtained, and the curve obtained from the intensity data did not overlap that of the lifetime data. They attributed the curvature of the Stern−Volmer plots to an inhomogeneous environment of the dye molecules in the system and the deviation between the two Stern−Volmer curves to static quenching.[42]

To develop a deeper understanding of the response of this system, Hartmann et al.[43] carried out new experiments, comparing the dye-plus-silica in the silicone resin with the dye itself in other media such as polystyrene. They fitted the nonexponential decay profiles to a double-exponential function and calculated mean decay times. In Figure 2, we present both the intensity and lifetime Stern−Volmer curves obtained from their data. The authors suggested that the nonlinearity of these Stern−Volmer plots indicates a microheterogeneity of binding sites for the probe molecules

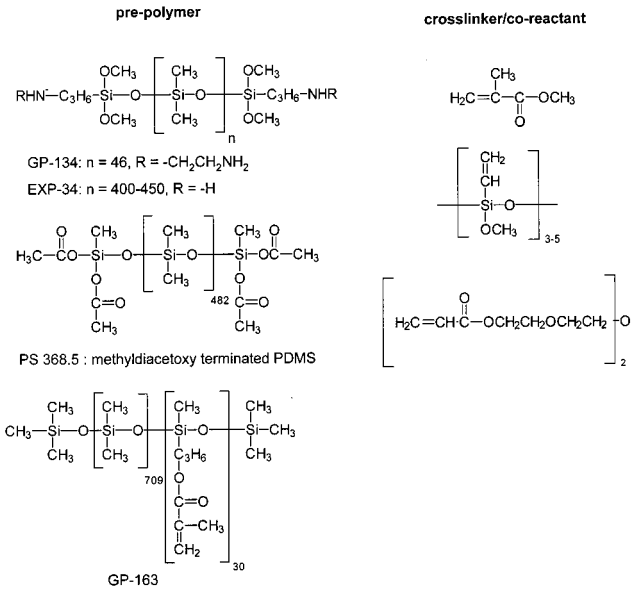

Figure 3. Chemical structures of the several silicone prepolymers used in experiments by Xu et al.[48] GP-134, EXP-34, and PS 368.5 were cured with atmospheric moisture at room temperature. The cross-linking of GP-164 requires reaction with one of the cross-linking agents shown in the figure. Copyright 1994 American Chemistry Society.

as well as the effect of an adsorption isotherm of oxygen on the silica surface. At the same time, Meier et al.[44] reported studies of a ruthenium dye in combination with a zeolite as the carrier pigment for sensor applications. They were able to prepare a silicone-based system in which the dye was encapsulated in the zeolite and also a system in which the dye was adsorbed onto the external zeolite surface. The latter system showed a higher quenching efficiency.

The Demas group[45] examined oxygen quenching of ruthenium dyes in RTV-118 silicone resin (General Electric, containing 10−30 wt % amorphous silica) and in other silicone matrixes and studied the effect of various ligands on the quenching properties of oxygen in the matrix. They also compared the effectiveness of oxygen quenching of the phosphorescence of ruthenium complexes in various media, including organic solvents[46] and solid silica gel.[47] A characteristic feature of their work is the use of silica with a hydrophobic surface. Xu et al.[48] described a broad series of experiments with various silicone polymers containing Cab-O-Sil TS-720 (Cabot Co., fumed silica particles with a surface area of 100 m^2/g and an average aggregate length of 200−300 nm). In this material, most of the SiOH groups have been replaced with $O[Si(CH_3)_2O]_n-Si(CH_3)_3$ groups. To prepare the samples, the silica was dispersed in the silicone polymer prior to cross-linking and then cured in place. These films were dipped into a solution of the dye in CH_2Cl_2. The films absorbed the dye and turned orange. Silica-free films were prepared similarly. For comparison experiments with the dye imbedded in solid silica, the particles were allowed to absorb dye from the CH_2Cl_2 solution. The silica was then dried to a powder and pressed into a film using an IR pellet maker at room temperature. Examples of the chemical structures of the commercial silicone resins they investigated are shown in Figure 3. The authors commented that they were unable to dissolve their $Ru(Ph_2phen)_3$ dye in linear

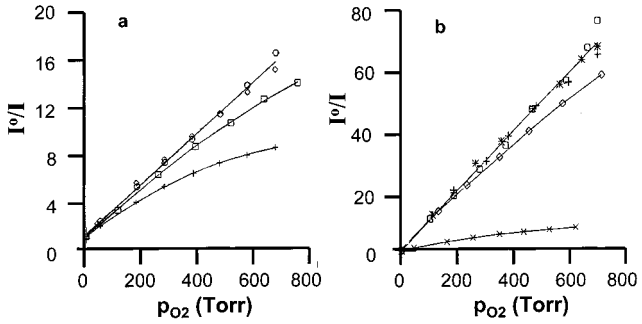

Figure 4. Intensity Stern−Volmer plots from ref 48 for Ru(Ph$_2$phen)$_3$Cl$_2$ in various media: (a) (+) GP-134, (□) EXP-34, (◇) GP-134 with 0.9 wt % silica, (○) GP-134 with 4.8 wt % silica; (b) (×) GP-134, (◇) PS-368.5, (+) PS 368.5 with 2 wt % silica, (*) PS 368.5 with 5 wt % silica, (□) hydrophobic silica disk. The chemical structures of these silicone resins are shown in Figure 3. Copyright 1994 American Chemistry Society.

PDMS, even when the counterion was changed to the very hydrophobic tetraphenyl borate anion. One can conclude that the polar groups in the cross-linked silicone resins play an important role in dye solubilization. Xu et al.[48] found very different Stern−Volmer behavior for the dyes in the different resins. An example is given in Figure 4. Some of the plots exhibit strong curvature. These are the types of data that the Demas group used to develop their ideas on the presence of multiple domains in the nanocomposite. Xu et al. commented that at least three types of domains exist, nonpolar PDMS domains, polar domains associate with the cross-linking sites, and the surfaces of the silica particles.

In the area of phosphorescence barometry, the oxygen-sensing matrix is applied as a coating to a model aviation or automotive part. In this type of application, there are two different types of motivation for the introduction of inorganic particles as fillers. The first stems from a desire to improve the mechanical properties of the polymer film. Cross-linking in silicone resins can have a number of unwanted consequences. Guillet[49] has commented that, when the cross-link density is low, the segmental motion of polymer chains is not strongly limited by those cross-links, and the diffusion of small molecules inside this polymer matrix show little effect from cross-linking. Commercial silicone resins, however, often have high cross-link densities. As the cure reaction proceeds, the diffusion of oxygen in the matrix can be affected significantly.[50] In addition, cross-linked resins are often difficult to remove when one wishes to reuse the model. On the other hand, linear polymers such as PDMS are viscoelastic fluids, and even very high molecular weight samples will flow when subjected to wind. Poly(*N*-alkylamino thionylphosphazenes) (C_n-PATP) developed by the Manners group[51−53] have a much smaller tendency to flow, but because of their low glass transition temperature (T_g), the polymer surface is tacky and tends to pick up dust in wind tunnel tests. The structure of C_4PATP is shown below in Figure 8b. Recent studies by Lu et al.[54] showed that the incorporation of 30 wt % of 10-nm-diameter hydrophobized silica particles (Nissan Chemical, Japan) into linear PDMS (M_w = 500 000, Polysciences) and 25 wt % of these particles into C_4PATP increased the stiffness and eliminated the tack of these coatings. These films, containing platinum octaethylporphine (PtOEP), remained void free and maintained a strong sensitivity to p_{O_2}.

Gouin and Gouterman[55] reported the addition of ball-milled aluminum oxide (Al_2O_3) with diameters ranging from 1 to 5 μm into a cross-linked silicone resin (SR-900, GE Silicones) containing platinum tetra(pentafluorophenyl)porphine (PtTFPP), in an effort to obtain robust PSPs. They studied the temperature dependence of the oxygen diffusion in these films by measuring the luminescence decays of the dye in filled polymer films with various filler concentrations.

One way to decrease the response time of particle-filled polymer films to a sudden change in p_{O_2}, and to modify their optical properties, is to add sufficient filler so that the polymer matrix contains voids. In the paint industry, the amount of inorganic pigment in a polymer is referred to as the pigment volume concentration (PVC). Above a critical pigment content (CPVC), there is no longer sufficient polymer to fill the gaps between the mineral particles, and voids appear. These voids scatter light, and the rate of oxygen diffusion through these voids is faster than the diffusion rate of oxygen through the polymer matrix. Thus, void-containing PSP formulations often have more intense signals, because of multiple scattering of the exciting light and the emitted light, and faster responses to changes in oxygen pressure.[56] Both Gouterman's group[57] and Sullivan's group[58] have reported that the introduction of high loadings of titanium oxide (TiO_2) can effectively decrease the response time of a PSP to a sharp pressure change. This decrease in response time was attributed to the presence a large fraction of microvoids inside the PSP films: Air can diffuse very rapidly to the inside of the coating through these voids. In addition, the effective thickness of the polymer phase is greatly reduced.

Whereas the blending of nanometer-sized silica particles with a polymer is one approach to prepare a polymer−inorganic hybrid material, an alternative approach is to use the sol−gel method in situ to generate a hybrid structure. Sol−gel-derived organic−inorganic nanocomposites have received a great amount of scientific and technological interest during the past decade.[59−61] The sol−gel technique also could be an effective approach to prepare nanocomposite sensing films. For example, Panusa et al.[62] investigated the sol−gel method to prepare a poly(methyl methacrylate)−silica nanocomposite film doped with 2-(5-amino-3,4,-dicyano-2H-pyrrol-2-ylidene)-1,1,2-tricyanoethanide, which can be used for sensing external species such as CN^- ions in water or NH_3 in air. One of the advantages of the sol-gel method is that the resulting inorganic and organic phases can have nanometer dimensions. In addition, changes in the reaction conditions can result in composites with different morphologies. At high pH, for example, one normally obtains discrete spherical silica particles, whereas at low pH, one obtains network-like silica structures interpenetrating the polymer matrix.

Effect of Inorganic Particles on Dye Spectroscopy. It is well-known that solvent polarity and the nature of local environments can have profound effects on the absorption and emission spectra of polar luminescent dye molecules. The effects are most pronounced

when the transition under consideration has substantial charge-transfer character. Many dyes have excited states with larger dipole moments than their ground electronic states. The solvent effect on emission is due to the relaxation of polar solvent molecules around the excited dye molecule, lowering the excited-state energy relative to the ground-state energy and leading to a shift in the emission spectrum to longer wavelength.[16] In polymer−filler composites, dye adsorption onto the mineral surface is accompanied by a change in environment. These surfaces are often more polar than that of the polymer matrix, and for many dyes, this can lead to a red shift in the dye emission. Another effect is possible. In solution, after excitation of a dye, solvent relaxation is rapid. For rigid systems such as glassy polymers or for dyes rigidly adsorbed onto a surface, this kind of solvation relaxation might be inhibited. The interaction of a dye with a solid surface can cause an enhancement of the luminescence quantum efficiency through the restriction of intramolecular rotation of the dye molecules.[63] In addition, the higher phosphorescence quantum yield shown by some luminescent dyes when they are adsorbed on solid surfaces might be attributed to the decreased efficiency of collisional quenching when both the dye and the quencher are adsorbed on the surface.[64,65]

Understanding the nature of spectral shifts of a dye at a surface is difficult. Attempts to describe these shifts (e.g., the Lippert equation[16]) in continuous media break down at interfaces because the parameters involved (dielectric constant, index of refraction) lose their meaning because they are macroscopic descriptions of a continuous medium. The particle surface can provide a range of sites, each with its own effect on the absorption and emission of light by the dye. If the polymer is in its glassy state, solvent relaxation around the dye might not occur on the time scale of the excited state.

For example, the polar surfaces of many fillers such as silica are able to solvate efficiently the charge-separated triplet metal-to-ligand charge-transfer (^{3}-MLCT) excited state of ruthenium dyes and lower its excited-state energy.[16,66] Carraway et al.[47] reported that $Ru(Ph_2phen)_3^{2+}$ shows similar absorption spectra in a Cab-O-Sil pressed disk and in methanol solution, except for some broadening in the spectrum of the ruthenium complex in methanol. The emission spectrum of three different ruthenium dyes differing in their ligands are all broad and structureless with maxima near 600 nm.[47] Whereas small shifts are seen in the emission spectra for $Ru(bpy)_3^{2+}$, the other dyes [$Ru(phen)_3^{2+}$ and $Ru(Ph_2phen)_3^{2+}$] show very similar spectra in methanol, pressed into a Ca-O-Sil disk, and dissolved in RTV-118 silicone resin. The implication of these spectra is that, in RTV-118, the dye molecules are adsorbed onto the surface of the silica particles present in the resin.

Much larger shifts were observed by Mingoarranz et al.[67] in the emission spectrum of $Ru(5\text{-odap})_3Cl_2$ (5-odap = 5-octadecanamide-1,10-phenanthroline) in different media. In a filler-free PDMS-based silicone resin, the emission consisted of a broad band with a maximum at 630 nm. Adsorbed to controlled-pore glass or hydrophilic silica in the silicone resin, the emission band was significantly narrower, with the maximum blue-shifted to 590 nm on controlled-pore glass (Sigma, 200−400 mesh, pore size 74 Å) and to 600 nm on silica gel (Whatman, with a surface area 350 m^2/g and a diameter of 5 μm). For dye molecules adsorbed on (hydrophobized) C_{18}−silica (Sigma), which has a surface area of 500 m^2/g and a particle size of 15−40 μm, they found a peak at 610 nm with a shoulder at 640 nm, suggesting two types of adsorption sites. Both these authors[67] and Carraway et al.[47] attributed the weaker sensitivity of $Ru(Ph_2phen)_3^{2+}$ to steric effects of the larger ligands, which, in their view, shield the excited state of the molecules from the local environment and make the complex largely insensitive to solvent variations.

Table 1. Parameters[a] for Oxygen Diffusion and Permeation in Silica-Filled and Unfilled C_4PATP Films

silica (wt %)	B ($I^o/I_{eq} - 1$)	$\langle\tau\rangle^o$ (μs)	$10^6\ D_{O_2}$[b]	$10^{12}\ P_{O_2,app}$[b] (from B)
0	60 ± 4	102.4 ± 0.4	3.7 ± 1.0	3.9 ± 0.4
10	55 ± 2	104.0 ± 0.1	3.0 ± 0.6[c] 5.3 ± 1.0[d]	3.5 ± 0.3
20	49 ± 3	104.5 ± 0.5	3.0 ± 0.8[c] 4.8 ± 0.5[d]	3.1 ± 0.3
25	50 ± 4	104.7 ± 0.3	2.7 ± 0.9[c] 3.9 ± 0.9[d]	3.2 ± 0.2

[a] From ref 54. [b] Units: D, $cm^2\ s^{-1}$, P, $mol\ cm^{-1}\ s^{-1}\ atm^{-1}$. [c] Diffusion coefficients obtained by fitting the oxygen-sorption intensity profiles. [d] Apparent diffusion coefficients obtained from the simulated intensity growth profile that best fits the data up to the midpoint of the oxygen desorption experiments.

Lu et al.[54] examined the influence of hydrophobized silica (Nissan Chemical, 10 nm diameter) on the absorption and emission spectra of platinum octaethylporphine (PtOEP) in two polymers, PDMS and poly(*n*-butylamino thionylphosphazene) (C_4PATP). PtOEP dissolves readily in both polymers. Excitation spectra showed that, in PDMS, with increased concentrations of silica nanoparticles, the excitation maximum shifted progressively to longer wavelengths. A corresponding progressive red shift was also observed in their emission spectra as the silica content of the composite was increased, and the bands became broadened. In striking contrast, PtOEP in C_4PATP exhibited no significant shift of the maximum positions in either excitation or emission spectra. Lu et al. explained this difference by inferring that, in PDMS, the dye molecules adsorb on the silica surface, whereas in C_4PATP, they do not adsorb but remain in the polymer. This conclusion is supported by the results of the luminescence decay measurements, in which the lifetimes of PtOEP in the absence of oxygen were measured in the two different types of polymer−silica composite films. The lifetime of PtOEP in PDMS−silica is strongly affected by the presence of silica, but that in C_4PATP−silica shows no change within experimental error as the concentration of silica is increased up to 25 wt % (see Table 1).

Oxygen Diffusion in Polymer−Mineral Composites

Oxygen diffusion in polymers normally follows Fick's Laws. In terms of the free volume model,[26] the diffusion of solutes such as oxygen in polymers occurs when density fluctuations associated with polymer segment or pendant group motion creates "holes" of sufficient size for the oxygen to move. Thermal expansion of the polymer upon heating increases the total free volume and promotes pendant group motion associated with the

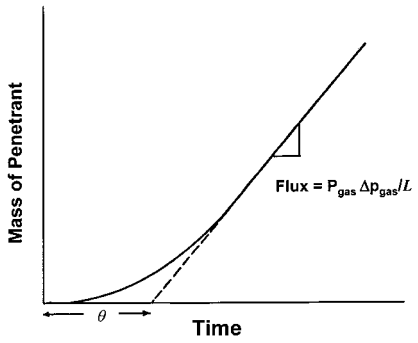

Figure 5. Typical membrane permeation response curve. Amount (mass or moles) of gas that passes through a polymer film of thickness L as a function of time. Extrapolation of the steady-state flux line to the time axis gives the time lag θ as the intercept.

β transition and backbone motion associated with the glass transition. The temperature dependence of diatomic gas diffusion above the glass transition temperature (T_g) of the polymer follows an Arrhenius behavior characterized by a small activation energy. It is sometimes argued[49] that gas diffusion in polymers is coupled to the motion of side or pendant groups of the polymer and, thus, that the temperature dependence is linked to the β relaxation of the polymer. If this point of view were rigorously correct, then one would see no change in the gas diffusion coefficient at T_g, which is sometimes found.

Gas Diffusion across Membranes. For more than 50 years, polymer scientists have been interested in the influence of fillers on gas diffusion through polymer membranes.[68] Gas transport is studied in a cell with two compartments separated by the polymer film of interest. In a typical experiment, both compartments are initially evacuated. At $t = 0$, the reservoir volume is charged with a gas at pressure p_{gas}, and gas transit through the membrane is monitored as an increase in pressure in the downstream compartment. The flux of gas is initially zero and then grows until it reaches its steady-state value, as shown in Figure 5. The diffusion coefficient of the gas (D_{gas}) is determined from the lag time θ, and the permeability of the gas P_{gas} is determined from the slope of the plot in the steady-state region of the flux, where Δp_{gas} is the pressure difference across the film of thickness L.

$$\theta = L^2/6D_{gas} \tag{6}$$

$$\text{slope} = P_{gas}\,\Delta p_{gas}/L \tag{7}$$

Paul and Kemp[69] point out that, when filler particles are present and act only as obstacles, the lag time θ increases and the steady-state flux is reduced. The filler effect on θ is more complicated than its effect on the steady-state flux. The complicating feature is that the gas might also adsorb onto the particle surface. Our analysis of this situation follows that of Paul and Kemp.

For diffusion in a polymer−filler composite, Fick's second law must be modified to take account of the concentration of adsorbed penetrant C_A

$$\frac{\partial C_{gas}}{\partial t} + \frac{\partial C_A}{\partial t} = D\,\frac{\partial^2 C_{gas}}{\partial x^2} \tag{8}$$

where eq 8 is written for unidimensional transport. Whereas the gas solubility C_{gas} follows Henry's Law ($C_{gas} = S_{gas}p_{gas}$), the adsorbed concentration more commonly follows a Langmuir adsorption isotherm

$$C_A = \frac{C_{max}bp_{gas}}{1 + bp_{gas}} \tag{9}$$

where C_{max} and b are the parameters in the Langmuir isotherm. When the membrane consists of a dispersed phase of an adsorptive filler with a volume fraction of ϕ_d and a polymeric continuous matrix of volume fraction of ϕ_p ($\phi_p = 1 - \phi_d$), the total concentration of gas, C, in the film at equilibrium is given by the sum of the Henry's law and Langmuir isotherm components.

$$C = \phi_p S_{gas} p_{gas} + \phi_d \frac{C_{max}bp_{gas}}{1 + bp_{gas}} \tag{10}$$

If the gas diffusion in the heterogeneous system can be treated as though it were occurring in a continuum with an effective diffusion coefficient of D_m, then the lag time for a conventional permeation experiment (Figure 5) is increased to

$$\theta_m = \frac{L^2}{6D_m}\left[1 + \frac{\phi_d}{\phi_p}Kf(y)\right] \tag{11}$$

with $K = C_{max}b/S_{gas}$, $y = bp_{gas}$, and

$$f(y) = 6y^{-3}[0.5y^2 + y - (1 - y)\ln(1 + y)]; \quad f(0) = 1; \quad f(\infty) = 0 \tag{12}$$

If the impermeable particles present in the composite film affect gas diffusion only by serving as obstacles, then D_m is proportional to the gas diffusion coefficient in the pure matrix phase[70]

$$D_m = \kappa D_{gas} \tag{13}$$

where κ is a structural factor that takes account of the geometric obstructions created by the filler. The same factor relates the permeability of the filled system, P_m, to that of the unfilled system,

$$P_m = \phi_p \kappa P \tag{14}$$

By eliminating κ from these expressions, one obtains

$$\frac{D_m}{D_{gas}} = \frac{P_m}{\phi_p P} \tag{15}$$

Thus, D_m values can be obtained using measured values of D_{gas}, P, and P_m. Paul and Kemp[69] review three models that attempt to relate the magnitude of κ to ϕ_p.

This analysis provides us with a number of important lessons for the effect of mineral fillers on the performance of oxygen sensors. First,the presence of the filler particles acting only as obstacles will have a relatively small effect on D_{O_2}. In steady-state permeation experiments, Van Amerongen[70] found that D_m values were never less than $0.75D_{gas}$ even for the most highly filled membranes. Second, transient experiments are predicted to show a much larger effect of the impermeable component on the oxygen diffusion rate. This effect arises from the adsorption of the oxygen on the surface

of the filler particles, and has a number of important consequences: (i) In response to an increase in the external oxygen partial pressure p_{O_2}, the approach to equilibrium will be retarded by gas adsorption onto the filler particles. (ii) If there is a significant binding energy of oxygen adsorption, the approach to equilibrium in response to a decrease in p_{O_2} will be strongly retarded. (iii) The total oxygen concentration in the composite will not increase linearly with p_{O_2}. As the external oxygen pressure is increased, the Henry's law solubility of the gas in the polymer matrix will continue to increase, but the surface adsorption on the filler particles will saturate. Paul and Kemp[69] mentioned that this type of behavior in a traditional membrane permeation experiment might lead one erroneously to infer that D_{gas} varied with pressure. (iv) Finally, one has to recognize that, in oxygen sensor experiments, the excited dyes sense only those oxygen molecules in their proximity. Dyes adsorbed on the filler particle surface will sense a different oxygen concentration than dyes in the polymer matrix.

In the arguments cited above, the filler particles act only as obstacles to increase the path length of molecules that diffuse across the membrane. In more global terms, one can imagine other mechanisms that affect gas diffusion rates through the influence of the filler surface on the segment mobility of polymer chains near the polymer−filler interface. There is evidence in the literature that, when the filler surface interacts strongly with the polymer, particle−surface interactions can lower the mobility of polymer molecules near the surface. Solid-state NMR experiments[71] and dielectric spectroscopy measurements[72] of silica−PDMS mixtures show that, if the silica surface is hydrophilic, an adsorption layer exists, approximately 1−2 nm in thickness, that has strongly reduced mobility compared to that of the bulk polymer. Dynamic-mechanical measurements from Eisenberg's group[73] indicate that surface interactions not only raise the glass transition of nearby polymer segments, but also reduce the total free volume in the polymer. There are also suggestions in the literature[74] that weakly interacting surfaces can increase the mobility of polymer segments near the surface. If gas diffusion in polymers is, in fact, sensitive to the free volume distribution in the matrix, then one would predict that polymer−surface interactions would affect gas diffusion rates. Here, the effect is on the friction coefficient experienced by the diffusant rather than on the tortuosity of the diffusion path.

Luminescence Detection of Oxygen Diffusion. In the experiments carried out by Cox and Dunn,[28−30] the values of D_{O_2} at room temperature (25 °C) in the silica-filled silicone films were obtained from the approach of the system to equilibrium upon exposure to an increase in external oxygen pressure. They found that these values decreased from 3.56×10^{-5} cm^2 s^{-1} for filler-free PDMS to 2.60×10^{-5} cm^2 s^{-1} for PDMS with 5 wt % silica (Figure 6). In light of the previous discussion, we now recognize that the D_{O_2} values that they determined in the presence of silica might contain contributions to the retardation from both obstacle effects of the filler and oxygen adsorption on its surface. The authors were particularly interested in the influence of temperature on the diffusion process. All of their samples

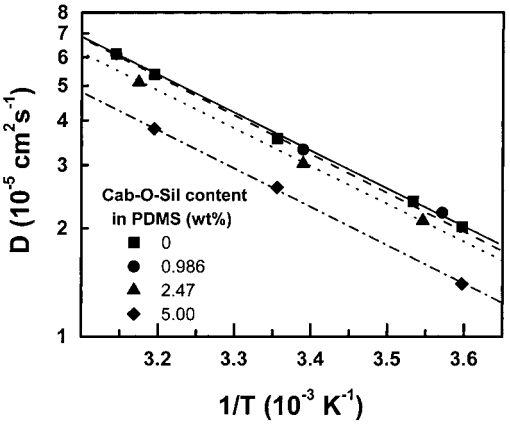

Figure 6. Arrhenius plots from ref 30 of log D_{O_2} versus $1/T$ for a silicone resin based on PDMS containing 1, 2.5, or 5 wt % Cab-O-Sil in which the D_{O_2} values were obtained from fluorescence quenching experiments. Copyright 1986 John Wiley & Sons, Inc.

showed an identical Arrhenius temperature-dependence of D_{O_2}, as shown in Figure 6. They concluded that the activation energy for oxygen diffusion remains unchanged for these various small silica concentrations.

Gouin and Gouterman[55] studied the temperature dependence of oxygen diffusion in silicone resins in the presence and absence of micrometer-sized Al_2O_3 particles by measuring the decay profiles of their luminescent dye PtTFPP. In these experiments, the authors did not determine D_{O_2} directly, but rather determined how the rate of oxygen diffusion changed through its influence on the quenching rate constant k_q. This approach requires a number of additional assumptions beyond those of the Cox and Dunn experiment.[30] In addition, it is sensitive to oxygen diffusion on a different length scale. In the Cox and Dunn experiment, oxygen diffusion is measured over a distance of millimeters and centimeters. In the time-resolved experiment, the characteristic length scale is $(6D\tau^o)^{1/2}$, i.e., on the order of 1 μm for $\tau^o \approx 100$ μs. Note also that each experiment is carried out at equilibrium with a fixed external oxygen partial pressure. Thus, the extent of oxygen adsorption on the Al_2O_3 during each measurement does not change.

In the analysis of their data, Gouin and Gouterman separate the radiative (k_r) and radiationless (k_{nr}) contributions to the excited-state decay, because the former does not depend on temperature. For an exponential decay process,[75] they write

$$\frac{1}{\tau} = \frac{1}{\tau^o} + k_q[O_2] = k_r + k_{nr} + k_q[O_2] \qquad (16)$$

Because the solubility of diatomic gases in condensed liquids or polymers is only weakly dependent on temperature,[76,77] they ignore temperature effects on $[O_2]$ and write an Arrhenius-type expression for k_q as

$$k_q[O_2] = A_q[O_2]\exp\left(-\frac{\Delta E_q}{RT}\right) = A_q'\left(-\frac{\Delta E_D}{RT}\right) \qquad (17)$$

where A_q is the preexponential constant of k_q and A_q' is the product of A_q and the O_2 concentration. The authors assume that the activation energy for oxygen quenching, ΔE_q, is equal to the activation energy for oxygen

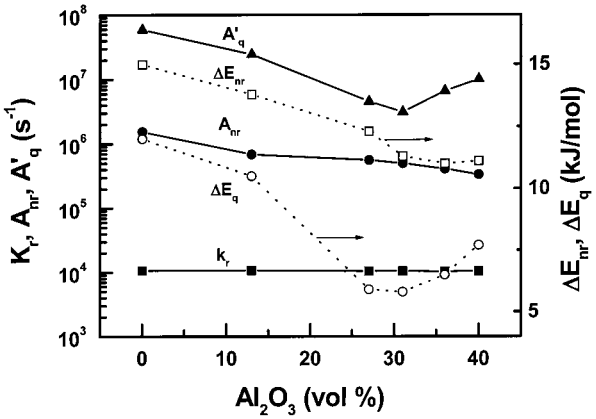

Figure 7. Plots of various parameters defined in the text as functions of the volume fraction of Al_2O_3 in a series of silicone−Al_2O_3 composite films from the luminescence decay measurements from ref 55.

diffusion, ΔE_D. These terms will be identical if α (eq 3) and $[O_2]$ do not change with temperature. They rewrite eq 17 as a function of temperature as

$$\frac{1}{\tau} = \frac{1}{\tau^o} + A_q'\left(-\frac{\Delta E_q}{RT}\right) = k_r + A_{nr}\exp\left(-\frac{\Delta E_{nr}}{RT}\right) + A_q'\left(-\frac{\Delta E_q}{RT}\right) \quad (18)$$

where A_{nr} is the preexponential term in the Arrhenius expression for k_{nr} and ΔE_{nr} is its activation energy.

Gouin and Gouterman carried out separate experiments in the presence and absence of oxygen for samples containing various amounts of filler. From the temperature dependence of τ^o, values of k_r, A_{nr}, and ΔE_{nr} were obtained. In the presence of oxygen, luminescence decays were not exponential. Mean decay times ($\tau \equiv \langle\tau\rangle$) were evaluated over temperatures ranging from 10 to 50 °C. These values were fitted to eq 18 to obtain values of A_q' and ΔE_q. In this way, Gouin and Gouterman could examine how all five fitting parameters varied with filler content for these Al_2O_3-containing resin films. They found that the parameters associated with the spectroscopy of the dye (k_r, A_{nr}, and ΔE_{nr}) do not vary significantly in the presence of Al_2O_3. ΔE_q values decrease slightly with increasing filler, whereas A_q' values decrease substantially, as shown in Figure 7, and pass through a minimum at a filler content near the CPVC. The increase in A_q' at higher filler content is likely to be due to the presence of voids in the composite.

The major focus of the Gouin and Gouterman paper was a search for a polymer−filler combination with a minimum temperature dependence of the luminescence intensity. Minimizing sensitivity to temperature is an essential feature of proper PSP design.[2] In this review, we are more concerned with the fundamental aspects of the quenching mechanism as it relates to oxygen diffusion in the matrix. Thus, we find it interesting that the ΔE_q values reported by Gouin and Gouterman[55] (pure resin, 12 kJ/mol; 13 vol % Al_2O_3, 10.5 kJ/mol) are significantly smaller than those reported by Cox and Dunn[28−30] (0−5 wt % silica, 20 kJ/mol). Assuming that the silicone resins themselves are not very different in composition, the 8 kJ/mol difference in activation energies points to a breakdown in some of the assumptions

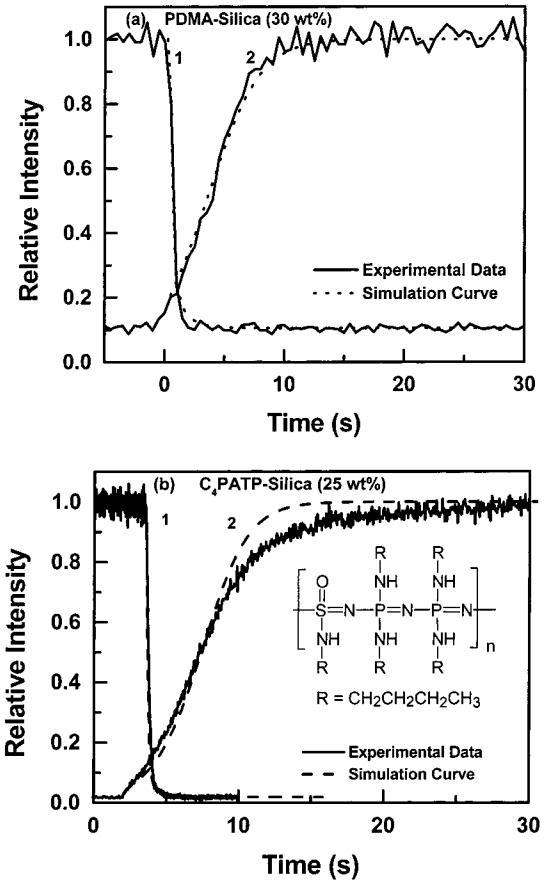

Figure 8. Plots of the luminescent intensity of PtOEP in a polymer composite film on glass as a function of time from ref 54. (a) PDMS−silica film (30 wt %, $L = 0.090$ mm). Curve 1, $D_{O_2} = 1.50 \times 10^{-5}$ cm^2 s^{-1}; curve 2, $D_{O_2} = 1.66 \times 10^{-5}$ cm^2 s^{-1}. (b) C_4PATP−silica film (25 wt %, $L = 0.043$ mm). Curve 1, $D_{O_2} = 2.7 \times 10^{-6}$ cm^2 s^{-1}; curve 2, $D_{O_2} = 3.9 \times 10^{-6}$ cm^2 s^{-1}.

in connecting the temperature dependence of quenching to the temperature dependence of macroscopic oxygen diffusion in a filler-free silicone resin. We also note that these authors did not explicitly consider the location of the dye in their composite and the possible role of adsorbed oxygen in their results.

Lu et al.[54] studied oxygen diffusion by phosphorescence quenching of PtOEP in linear PDMS and C_4PATP films containing up to 30 wt % (16 vol %) silica in the form of 10-nm particles with a hydrophobic surface. Although the dye dissolves easily in both polymers, once the silica is added, the composites differ in a key respect. In PDMS, the dye becomes bound to the surface of the silica, whereas in C_4PATP, it remains almost entirely in the polymer. Lu et al. determined D_{O_2} values by measuring the rate of change in the luminescence intensity of a polymer film under steady illumination with exposure to a sudden change of the oxygen pressure. In the oxygen sorption experiments, the nitrogen atmosphere was replaced by air (curve 1 in Figure 8a), and the intensity decreased. In the oxygen desorption experiments, the air atmosphere was replaced by nitrogen (curve 2 in Figure 8a), leading to an increase in the measured phosphorescence intensity. The data were fitted to simulated curves based on Fick's Law and Stern−Volmer quenching in which D_{O_2} was the only fitting parameter.[21] In a well-behaved system, such as the filler-free polymer, both oxygen sorption and de-

Table 2. Parameters for Oxygen Diffusion and Permeation Obtained from Time-Scan Experiments on Silica-Filled and Unfilled PDMS Films[a]

silica (wt %)	B ($I^o/I_{eq} - 1$)	$\langle\tau\rangle^o$ (μs)	$10^5\ D_{O_2}$[b]	$10^{12}\ P_{O_2,app}$[b] (from B)
0	176 ± 16	65 ± 4	2.2 ± 0.2	18 ± 2[c]
5	45 ± 8	78 ± 1	1.8 ± 0.2	3.8 ± 0.7
10	30 ± 4	84 ± 2	1.8 ± 0.1	2.4 ± 0.3
20	11 ± 3	96 ± 2	1.7 ± 0.2	0.76 ± 0.21
30	9 ± 3	91 ± 1	1.4 ± 0.2	0.65 ± 0.22

[a] From ref 54. [b] Units: D, $cm^2\ s^{-1}$; P, $mol\ cm^{-1}\ s^{-1}\ atm^{-1}$; apparent P values when silica is present. [c] For PDMS in the absence of silica, $S_{O_2} = (8.2 \pm 1.1) \times 10^{-4}$ M atm^{-1}.

sorption experiments give nearly identical values of D_{O_2}. The characteristic diffusion length scale of the experiment is the film thickness, ~0.1 mm. Although the data analysis did not take explicit account of oxygen adsorption onto the silica particles present in the system, the results left no doubt that this effect was an important contributor to their observations. In PDMS, where the dyes were strongly adsorbed onto the silica surface, the experiment followed Fick's law (see Figure 8a) and gave D_{O_2} values that decreased as the silica content was increased from $D_{O_2} = 2.2 \pm 0.2 \times 10^{-5}\ cm^2\ s^{-1}$ in the absence of silica to $1.8 \pm 0.2 \times 10^{-5}\ cm^2\ s^{-1}$ at 5 wt % and $1.4 \pm 0.2 \times 10^{-5}\ cm^2\ s^{-1}$ at 30 wt % (Table 2). The magnitude of the change observed for 5 wt % silica was similar to that found by Cox and Dunn.[30] Experiments with C_4PATP were more complicated. The PtOEP dye in this polymer does not adsorb onto the silica but remains free in the polymer matrix. In Figure 8b, one sees that the measured increase in intensity as oxygen diffuses out of the filled polymer initially increases faster than that predicted for a D_{O_2} value of $3.9 \times 10^{-6}\ cm^2\ s^{-1}$ and then exhibits a long tail in the intensity-growth curve. The authors explain this unexpected behavior in the following way. Whereas the PtOEP dye does not adsorb onto the silica in this matrix, oxygen molecules do adsorb. Unlike the case of PtOEP in PDMS−silica, the oxygen molecules on the silica surface do not participate in quenching. In the desorption experiment, the silica surface acts as a reservoir for oxygen, which bleeds slowly off the surface as oxygen diffuses out of the C_4PATP matrix and into the surrounding atmosphere. Much smaller deviations are seen in the corresponding experiment for oxygen diffusion into the C_4PATP matrix containing 25 wt % silica particles, giving an apparent D_{O_2} value of $2.7 \times 10^{-6}\ cm^2\ s^{-1}$. This compares to a D_{O_2} value of $3.7 \pm 1.0 \times 10^{-6}\ cm^2\ s^{-1}$ in the absence of silica (Table 1).

Oxygen Solubility in Polymer−Mineral Composites

As we have seen in the previous section, in the presence of filler, the total concentration of oxygen in the matrix has two contributions, the Henry's law solubility of oxygen in the polymer plus an isotherm describing oxygen binding to the filler surface (see eq 10). A similar sorption model is necessary to describe gas sorption into glassy polymers.[78] For filler-free polymers at $T < T_g$, gas solubility does not follow Henry's law; rather, two parameters are needed to describe the pressure dependence of the oxygen solubility. In the dual-mode sorption model, one assumes that the penetrant gas molecules are distributed in two distinct populations or sites in the polymer: (a) Henry-type dissolution (random mixing, weak interactions with the polymer) in which the penetrant concentration increases linearly with the pressure and (b) Langmuir-type sorption (sorption into sites of excess of unrelaxed free volume, strong interactions with the polymer).

We know of few papers in which measurements of gas sorption have been carried out on polymer−filler composites. Paul and Kemp[69] used a microbalance to measure gas uptake in a polymer membrane containing molecular sieves as the filler. They intended to use this information to account quantitatively for the filler effect on the time lag in membrane diffusion experiments. More recently, Kamiya et al.[79] determined adsorption, desorption, and dilation isotherms for seven gases including oxygen in two different polymer matrixes. One was a linear PDMS liquid. The second was in a cross-linked silicone containing 29 wt % silica (precipitated silica, Nippon Silica Industrial Co., 8 to 16 μm particles). Whereas the PDMS showed Henry's law behavior over a large pressure range, the filled silicone resin exhibited dual-mode sorption analogous to that described by eq 10. From the dilation experiments, they obtained the partial molar volume of each gas in the polymer matrix and were able to show that the gas adsorbed on the silica surface did not lead to an increase in the polymer volume. One of their striking observations was the hysteresis seen in the sorption vs desorption isotherms for O_2. The authors argued that the origin of this hysteresis seen for O_2 is strong interactions between the oxygen molecules and specific adsorption sites on the silica surface. Joly et al.[80,81] used a dual-mode model to describe the oxygen isotherm in a silica−polyimide hybrid system. In their experiments, they found an increase of oxygen permeation after the introduction of silica.

We now examine how these effects are manifest in oxygen sensor experiments. In the experiments by Lu et al. shown in Figure 8, equilibrium values of I^o/I_{air} can be obtained from the limiting intensities from each film before and after exposure to a change in atmosphere. Thus, the B values (defined as $I^o/I_{0.21atm} - 1$ when $p_{O_2} = 0.21$ atm) determined in the presence and absence of silica should allow for corresponding P_{O_2} values to be calculated according to eq 5. Although this approach works well in the absence of filler, it breaks down when silica is present. As shown in Table 1, values of B decrease substantially as the silica content of the polymer is increased, leading to the unreasonable deduction that silica causes a large decrease in oxygen permeability while causing much smaller changes in oxygen diffusivity. Pulsed laser experiments show that, although the phosphorescence decay of PtOEP in the absence of oxygen is exponential (with a lifetime that increases in the presence of silica), the combination of silica plus oxygen leads to strongly nonexponential decays. Lu et al. commented that values of $\tau^o/\langle\tau\rangle$ (where $\langle\tau\rangle$ is the mean decay time) are very different from I^o/I_{air}, a second indication that the assumptions leading to eq 5 no longer hold in the presence of the silica particles. These experiments, together with those involving C_4PATP plus silica, led the authors to conclude that oxygen adsorption on silica plays an important role

in the experiment. In their experiments, with the data available, this adsorption was difficult to quantify, and it has not been taken into account in any of the oxygen diffusion experiments described in the preceding section.

There are examples in the analytical chemistry literature where authors have considered oxygen and dye adsorption onto silica to explain deviations from simple Stern−Volmer quenching data. Hartmann et al.[43] pointed out that it is reasonable to consider the application of a dual-mode model in a silicone−silica system. Unfortunately they had insufficient data to test this idea and did not attempt to measure the oxygen sorption isotherm directly. Instead, they used a "two-site" model to fit their results of Stern−Volmer plots. In the two-site model, one imagines that there are two types of sites that contribute to quenching, each with its own Stern−Volmer constants. More complex behavior, such as heterogeneous binding of the dyes and oxygen to the silica particle could also give nonlinear Stern−Volmer plots.

Lippitsch et al.[82] developed a more sophisticated model to describe the nonexponential decay profiles of ruthenium dyes in polymer matrixes and to explain nonlinear Stern−Volmer plots. Their model is based on a Förster-type energy transfer[83] between dye molecules in different environments, leading to a stretched exponential function for the decay curve profile.

The Demas group[47] compared the oxygen quenching of ruthenium complexes in organic solvents, in a disk pressed from hydrophobized silica, and in RTV-118 silica-containing resin. They proposed several quenching mechanisms: surface quenching, a two-site model, and a combination of surface quenching and a two-site model. Judging from the curvature in the Stern−Volmer plots, they preferred for the data in RTV-118 a model with two independent sites each with a different quenching constant. For oxygen quenching of the dyes incorporated into the silica disk, they considered a surface-quenching model with a Freundlich isotherm rather than a Langmuir isotherm. The Langmuir model assumes that all sites have the same binding energy, whereas the Freundlich model acknowledges that there can be a distribution of site energies with preferential binding to the most energetic sites.[47,84] The Freundlich adsorption isotherm can be expressed as

$$\frac{C_A}{C_{max}} = a p_{O_2}^{1/n} \tag{19}$$

where a is a collection of constants and n is an empirical parameter related to the intensity of the adsorption. Stern−Volmer plots by themselves do not provide sufficient data to characterize the nature or extent of oxygen adsorption on the filler particles.

Mingoarranz et al.[67] also invoked the idea that oxygen adsorption on polar surfaces plays an important role in oxygen quenching in composite sensors. They found strongly enhanced sensitivity to quenching when dyes adsorbed to strongly polar surfaces (controlled pore glass, hydrophilic silica gel) were present in significant amounts in their sensors.

We know of no data on the temperature effects of oxygen adsorption on mineral surfaces in mineral−polymer composites. Krasnansky et al.[85] measured the

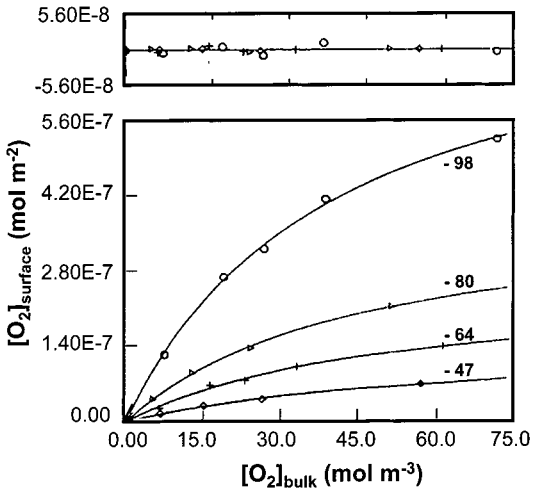

Figure 9. Oxygen adsorption isotherms on Cab-O-Sil (separated points) along with the simulation according to Langmuir model (continuous lines) at various temperatures from ref 85. Copyright 1990 American Chemistry Society.

temperature dependence of oxygen adsorption at the gas−silica surface using a hydrophilic fumed silica (Cab-O-Sil HS-5, Cabot), which has a surface area of 325 m^2/g and a particle diameter of 0.008 mm. They found that oxygen adsorption on the silica gas/solid interface followed a Langmuir-type isotherm at various temperatures up to −47 °C and that the amount of oxygen adsorbed increased as the temperature decreased (Figure 9).

They gave an expression for the temperature dependence of the term b in the Langmuir isotherm (eq 9) as

$$\ln b + \ln [O_2]_{ads,M} = \ln\left[\frac{1}{k^o}\left(\frac{k_B}{2\pi m_w}\right)^{1/2}\right] - 0.5 \ln\left(\frac{1}{T}\right) + \frac{\Delta E_{ads,L}}{RT} \tag{20}$$

where k^o is a frequency factor, m_w is the molecular weight of oxygen, and $\Delta E_{ads,L}$ is the heat of adsorption. This equation can be rearranged to eq 21 by collecting all of the temperature-independent parameters into a preexponential term, A_b. The subscript L refers to a Langmuir-type isotherm.

$$b = \frac{A_{b,L}}{\sqrt{T}} \exp\left(-\frac{\Delta E_{ads,L}}{RT}\right) \tag{21}$$

From computer simulations, they found that b increased almost exponentially with $1/T$. Recalling that the amount of oxygen dissolved in a polymer phase according to Henry's law is only weakly temperature-dependent, one would see a significant effect of temperature on the solubility of oxygen in a polymer−mineral composite if this strong temperature dependence persisted for mineral fillers in a polymer matrix. Sakaue et al.[86] argued that a Freundlich-type isotherm will have a somewhat similar temperature dependence

$$b = \frac{A_{b,F}}{\sqrt{T^r}} \exp\left(-\frac{\Delta E_{ads,F}}{RT}\right) \tag{22}$$

Oxygen Quenching of Dyes Bound to Silica

As mentioned in the preceding section, some authors have attempted to develop models for luminescence

quenching in polymer nanocomposite films based on the ideas of multiple sites where quenching can occur.[87] The simplest such model is the two-site model, which, in its most basic form, assumes that the oxygen concentration is uniform but that the lifetimes and quenching constants are different

$$\frac{I^o}{I} = \left(\frac{f_{01}}{1 + K_{SV1}[O_2]} + \frac{f_{02}}{1 + K_{SV2}[O_2]}\right)^{-1} \qquad (23)$$

where f_{0i} is the steady-state or integrated fraction of light emitted from the ith component and K_{SVi} is its Stern−Volmer constant. When all quenching is dynamic, K_{SVi} is the product of k_q and the unquenched lifetime τ^o at each site. Demas et al. extended this model to the case in which there are more than two emitting sites with different quenching constants.[47] As a consequence

$$\frac{I^o}{I} = \left(\sum_i^n \frac{f_{0i}}{1 + K_{SVi}[O_2]}\right)^{-1} \qquad (24)$$

In the multisite model, each decay curve will be a sum of exponential terms. If the emission spectra from the different sites are the same and the radiative rate constant for all sites are the same, then the sample impulse response is given by

$$i(t) = \sum_j (f_{0j}/\tau_{0j}) \exp(-t/\tau_j)$$

$$\tau_j = \tau_{0j}/(1 + K_{SVj}[Q]) \qquad (25)$$

In the analytical chemistry literature, most of the publications on polymer−mineral composites as oxygen sensors report only intensity Stern−Volmer plots as the data and use models such as those in eqs 23 and 24 to rationalize curvature in the Stern−Volmer plots. We know of no examples other than that of Gouin and Gouterman[55] where extensive lifetime measurements have been carried out. Up to now, there have been no investigations of these systems in sufficient detail to begin to unravel the details of the quenching kinetics.

Wolfbeis et al.[40,42] and Hartmann et al.[43] described lifetime and intensity measurements for $Ru(Ph_2phen)_3^{2+}$ as the dye in a cross-linked silicone polymer. Hartmann et al. fitted their decay profiles to a sum of two exponential terms ($\tau_{long} = 1.6$ μs, $\tau_{short} = 0.78$ μs in nitrogen, Figure 2). One of the differences between their system and those of Lu et al.[54] and Gouin and Gouterman[55] is the choice of dyes. The latter two groups use nonionic porphyrin dyes, which have the simplifying feature that they exhibit simple exponential decay profiles in the absence of oxygen, even in the presence of mineral fillers. These types of dyes can help one sort out the difference between a heterogeneous distribution of dye binding sites and a distribution of oxygen binding sites in a system. Hartmann et al.[43] explicitly raised their understanding that oxygen adsorption onto the silica and its surface diffusion play an important role in the observed quenching. Their data do not allow them to unravel the competing contributions of quenching in the polymer matrix and quenching on the silica surface. The authors conclude that their results provide strong evidence for the presence of a microheterogeneity of binding sites in their system.

The situation is different in the case of experiments involving dyes bound to the surface of silica and exposed to quenchers either in the gas phase or in a simple liquid medium in which the silica particles are dispersed. Here, a much deeper analysis of the fluorescence quenching data has been carried out. When the quencher is initially in the gas phase, aspects of the quenching mechanism can be different. For example, the excited dye could be quenched through a direct encounter with an oxygen molecule that has diffused through the gas phase. This process is known as the Eley−Rideal (ER)[88] mechanism. Alternatively, oxygen gas can adsorb reversibly onto the surface and then diffuse along the surface until it encounters an excited dye. This mechanism is known as the Langmuir−Hinshelwood (LH)[89] mechanism. Both mechanisms can operate simultaneously. When the oxygen adsorption is small, the dominant mechanism will involve direct collisions from the gas phase.

Temperature can play an important role in determining the dominant quenching mechanism. In his review article, Thomas[90] points out that, because oxygen adsorption onto the bare silica surface is exothermic, it will be favored at lower temperatures. In both mechanisms, k_q will increase with increasing temperature because of thermally activated oxygen diffusion in the gas phase or on the surface. Reactions that follow the LH mechanism will decrease in importance at elevated temperature, as the surface coverage of oxygen will decrease. One would expect a curved plot of log k_q vs $1/T$ when the two mechanisms operate simultaneously.[91] Thus, the temperature dependence of the quenching kinetics can provide useful information about the quenching mechanism.

The simplest expression of the competing ER and LH mechanisms assumes that all dye molecules on the surface have the same unquenched lifetimes.[92]

$$\frac{1}{\tau} = \frac{1}{\tau^o} + k_{ER}[O_2] + k_{LH}[O_2]_{ads} \qquad (26)$$

Here, k_{ER} is the quenching rate constant for the ER mechanism and $[O_2]$ is the molar concentration of oxygen in gas phase; k_{LH} is the quenching rate constant due to the surface diffusion mechanism, and $[O_2]_{ads}$ is the surface molar concentration of adsorbed oxygen. The simple ER collision theory predicts that the bimolecular collisional quenching rate for reaction with oxygen should be proportional to the frequency of surface collisions. The collisional frequency per unit area is predicted to increase with the square root of the absolute temperature. In the LH mechanism, Freeman and Doll[93,94] point out that one needs to consider the diffusion coefficient of oxygen on the mineral surface, D_{s,O_2}.

$$k_{LH} = 2\pi\sigma D_{s,O_2}\lambda_0 \qquad (27)$$

where σ has the same meaning as in eq 4 and the parameter λ_0 is related to the distance an oxygen molecule will diffuse during its mean residence time on the surface.

Table 3. Classification of Dynamic Quenching Processes and Notation for the Corresponding Rate Constant

type	dynamic quenching process	rate constant
i	O_2 (polymer) + dye* (polymer) →	k_q
ii	O_2 (polymer) + dye* (silica) →	k_{ER}
iii	O_2 (silica) + dye* (silica) →	k_{LH}
iv	O_2 (silica) + dye* (polymer) → O_2 (polymer) + dye* (polymer) →	$k_{q,c}$

Drake et al.[95] studied the phosphorescence quenching of benzophenone on microporous silica monitored by time-resolved diffuse-reflectance measurements. From a comparison of the quenching rate and the adsorption isotherm for oxygen, they deduced that quenching was entirely from the gas phase with no surface diffusion. Oxygen quenching experiments by Levin et al.[96] of zinc tetraphenylporphyrin on silica and by Springob and Wolff[97] of fluoranthene on silica were both interpreted in terms of quenching that followed a Langmuir−Hinshelwood mechanism. The apparent contradiction between these different experiments might point to the influence of the nature of the silica surface on the quenching mechanism.

The J. K. Thomas group has carried out extensive studies of oxygen quenching of singlet excited pyrene on silica and on alumina.[85,98,99] They measured both spectra and fluorescence decay profiles. Taking eq 26 as their basis, they analyzed nonexponential pyrene decay profiles in terms of a Gaussian distribution of pyrene decay rates on the mineral surface. In this way, they simplified the curve fitting to two meaningful parameters, the mean decay rate and the breadth of the decay rate distribution. In analyzing their data, they found an important role for adsorbed oxygen in the quenching process. In reporting their study of oxygen quenching at the silica/gas interface, Krasnansky et al.[85,100] commented that the silica surface plays a role in the quenching mechanism analogous to that of a solvent cage in solution. The interaction time of the surface-bound dye molecules and quencher is prolonged, and the excess translational, vibrational, and rotational energies of the oxygen are dissipated by the adsorption process. Thus, the adsorption process increases the quenching probability.

There are also many studies of oxygen quenching of surface-immobilized ruthenium complexes.[47,66,101−103] Avnir's group found that the mechanism of oxygen quenching of $Ru(bpy)_3^{2+}$ on silica depends on oxygen coverage of the silica as well as the temperature. They concluded that both the ER and LH mechanisms are involved.[101,102]

Some authors have studied the luminescence quenching of dyes bound to mineral particles by quenchers dissolved in a solvent. Wong et al.[104,105] studied fluorescence quenching from pyrene groups covalently bound to the surface of porous silica by the reaction of Si−OH groups on the silica with 3-(1-pyrenyl) propyldimethylchlorosilane (3PPS). They examined iodine as the quencher using a series of primary alcohols as solvents. The iodine quencher is not significantly adsorbed to the silica surface in these solvents. Thus, the quenching occurs through collisions between iodine molecules in the solvent and 3PPS on the surface. They found that the quenching of 3PPS follows simple exponential decay kinetics and linear Stern−Volmer behavior, which indicates that the diffusion of small molecules is the rate-determining step. Thus, quenching appears to follow a simple ER mechanism.

Summary

Dye-containing polymer−mineral nanocomposites have useful properties as luminescent oxygen sensors. The mineral phase improves the mechanical properties of the material and can serve as a carrier for the dye. Composites containing mineral above the critical pigment volume composition are porous. This porosity facilitates oxygen penetration into the structure, thus improving the response time of the material to a rapid change in oxygen pressure. At the same time, the porosity leads to multiple scattering in optical experiments, which might be useful in increasing the signal intensity in luminescence detection experiments.

To design optimum sensors, one needs to understand the factors that affect the interaction of excited dyes in these systems with oxygen. Given the complexity of the issues raised in the preceding sections of this paper, developing this kind of understanding remains a challenge. The first set of issues one has to address are the locus of the dye and its state of aggregation. Depending on the structure of the dye, the chemical structure of the polymer, and the nature of the surface of the inorganic filler, the dye can be dissolved in the polymer, adsorbed molecularly on the filler surface, or present as dimers or aggregates on the filler particle surface. It is not easy to characterize this state of the system. Even for the dye itself in the polymer, particularly for ionic dyes in nonpolar polymer films, it can be difficult to determine whether the dye is dissolved or present as small aggregates. The second issue that one should address is the location of oxygen in the system. For polymers above T_g, one needs the Henry's Law solubility of oxygen in the polymer plus the binding isotherm for oxygen on the surface of the inorganic particles while dispersed in the polymer. We know of only one example[79] in which this type of information on oxygen adsorption has been obtained. One imagines that the nature of this binding capacity for oxygen will depend on the nature of the particle surface as it is affected by interaction with the polymer medium.

From a spectroscopic point of view, one needs information about the unquenched decay rate of the dye, particularly whether it can be characterized by a single-exponential term or a distribution of exponentials. Here, one can be guided by the approach of J. K. Thomas and co-workers,[85] who treat the unquenched pyrene emission from the surface of silica particles as a Gaussian distribution of exponentials.

Finally, one has to try to sort out the various quenching processes that take place in the system. One has first to distinguish between dynamic quenching and static quenching. Static quenching is the term used to describe the situation in which the quencher is next to the chromophore at the moment of excitation, so that

quenching occurs without the need for diffusion. Because this quenching is normally very rapid (picoseconds or faster), dyes that are quenched in this way make no contribution to measured luminescence decay profiles. Thus, static quenching can be identified by changes in I that are not reflected in τ. In Table 3, we list four general scenarios that can contribute to dynamic quenching in a polymer−filler nanocomposite. In the polymer phase (case i), one has the type of quenching described by eqs 1−5 in the Quenching Kinetics section of this paper. Case ii corresponds to the Eley−Rideal quenching of surface-bound dyes by quenchers diffusing through the external medium. Case iii describes the Langmuir−Hinshelwood mechanism in which O_2 molecules adsorb to the particle surface prior to quenching a dye on the surface. Finally, case iv describes the situation inferred for PtOEP + silica in C_4PATP, where oxygen bound to the silica surface does not participate in quenching until it desorbs from the surface and interacts with an excited dye in the polymer phase.

In the current state of the art, we are far from obtaining this kind of detailed information about luminescence quenching in any organic−inorganic nanocomposite. Significant progress has been made in understanding fluorescence and phosphorescence quenching kinetics for polymer media and for inorganic nanoparticles in air with dyes bound to their surface. We anticipate that future experiments will take us closer to the goal of a molecular understanding of luminescence quenching processes in composite media. Nevertheless, it is important to realize that some systems will be subject to complexities beyond those listed above. For example, groups at the mineral surface can react over time with moisture or with groups on the polymer chain.[106] Experiments with polymers in the glassy state ($T < T_g$) will introduce additional phenomena into the problem, ranging from dual-mode gas sorption to time- and temperature-dependent physical relaxation of the polymer matrix.

Acknowledgment. The authors thank NSERC Canada and Materials and Manufacturing Ontario (MMO) for their support of this research.

References

(1) Demas, J. N.; DeGraff, B. A. *J. Chem. Educ.* **1997**, *74* (6), 690.
(2) Gouterman, M. *J. Chem. Educ.* **1997**, *74* (6), 697.
(3) Liu, T.; Campbell, B. T.; Burns, S. P.; Sullivan, J. P. *Appl. Mech. Rev.* **1997**, *50*, 227.
(4) Moshasrov, V.; Radchenko, V.; Fonov, S. *Luminescent Pressure Sensors in Aerodynamic Experiments*; Central Aerohydrodynamic Institute (TsAGI): Moscow, Russia, 1998.
(5) Lu, X.; Winnik, M. A. Luminescence Quenching in Polymer Films. In *Molecular and Supramolecular Photochemistry*; Ramamurthy, V., Schanze, K. S., Eds.; Marcel-Dekker: New York, 2000; Vol. 6, pp 311−352.
(6) Demas, J. N.; DeGraff, B. A. Design and Applications of Highly Luminescent Transition Metal Complexes. In *Topics in Fluorescence Spectroscopy*; Lakowicz, J. R., Ed.; Plenum Press: New York, 1994; Vol. 4. Probe Design and Chemical Sensing, pp 71−107.
(7) Wolfbeis, O. S. Oxygen Sensors. In *Fiber Optic Chemical Sensors and Biosensors*; Wolfbeis, O. S., Ed.; CRC Press: Boca Raton, FL, 1991; Vol. 2, pp 19−54.
(8) Bell, J. H.; Schairer, E. T.; Hand, L. A.; Mehta, R. D. *Annu. Rev. Fluid Mech.* **2001**, *33*, 155−206.
(9) Ji, H. F.; Shen, Y.; Hubner, J. P.; Carroll, B. F.; Schmehl, R. H.; Simon, J. A.; Schanze, K. S. *Appl. Spectrosc.* **2000**, *54* (6), 856−863.
(10) Oglesby, D. M.; Puram, C. K.; Upchurch, B. T. *NASA Technical Memorandum 4695*; Goddard Space Flight Center: Greenbelt, MD, 1995.
(11) Nielsen, L. E.; Landel, R. F. *Mechanical Properties of Polymers and Composites*; Marcel Dekker: New York, 1994.
(12) Mark, J. E. *Polym. Eng. Sci.* **1996**, *36*, 2905.
(13) *Polymer-Based Molecular Composites: Materials Research Society Symposium Proceedings*; Schaefer, D. W., Mark, J. E., Eds.; Materials Research Society: Pittsburgh, PA, 1990.
(14) *Particulate-Filled Polymer Composites*; Rothon, R., Ed.; Wiley: New York, 1995.
(15) In contrast, static quenching refers to the situation in which neither the excited dye nor the quencher has significant mobility on the time scale of the excited state. Static quenching can be described by the Perrin model.[16]
(16) Lakowicz, J. R. *Principles of Fluorescence Spectroscopy*; Kluwer Academic/Plenum Publishers: New York, 1999.
(17) Mills, A. *Sens. Actuators B* **1998**, *51*, 60.
(18) Turro, N. J. *Modern Molecular Photochemistry*; Benjamin-Cummings: Menlo Park, CA, 1978; pp 590−591.
(19) Chu, D. Y.; Thomas, J. K.; Kuczynski, J. *Macromolecules* **1988**, *21*, 2094.
(20) Nowakowska, P. F.; Najbar, J.; Waligora, B. *Eur. Polym. J.* **1976**, *12*, 387.
(21) (a) Yekta, A.; Masoumi, Z.; Winnik, M. A. *Can. J. Chem.* **1995**, *73*, 2021. (b) The very different time scales for sorption and desorption kinetics seen in Figure 8 are predicted by the theory that couples Fickian diffusion with Stern−Volmer quenching kinetics, as shown in ref 21a.
(22) (a) Gijzeman, O. L. J.; Kaufman, F.; Porter, G. J. *Chem. Phys. Lett.* **1970**, *69*, 708. (b) Patterson, L. K.; Porter, G.; Topp, M. R. *Chem. Phys. Lett.* **1970**, *7*, 612. (c) Guillet, J. E.; Andrews, M. *Macromolecules* **1992**, *25*, 2752.
(23) Demas, J. N.; Harris, E. W.; McBride, R. P. *J. Am. Chem. Soc.* **1977**, *99*, 3547.
(24) Collins, F. C.; Kimball, G. E. *J. Colloid Sci.* **1949**, *4*, 425.
(25) Smoluchowski, M. *J. Phys. Chem.* **1917**, *92*, 129.
(26) Guillet, J. E. In *Photophysical and Photochemical Tools in Polymer Science*; Winnik, M. A., Ed.; NATO ASI C182; D. Reidel: Dordrecht, The Netherlands, 1986; pp 467−494.
(27) Crank, J.; Park, G. S. In *Diffusion in Polymers*; Crank, J., Park, G. S., Eds.; Academic Press: New York, 1968; pp 1−39.
(28) Cox, M. E.; Dunn, B. *J. Polym. Soc. A: Polym. Chem.* **1986**, *24*, 621.
(29) Cox, M. E.; Dunn, B. *Appl. Opt.* **1985**, *24*, 2114.
(30) Cox, M. E.; Dunn, B. *J. Polym. Sci. A: Polym. Chem.* **1986**, *24*, 2395.
(31) Wang, B.; Ogilby, P. R. *Can. J. Chem.* **1995**, *73*, 1831.
(32) Gao, Y.; Baca, A. M.; Wang, B.; Ogilby, P. R. *Macromolecules* **1994**, *27* (24), 7041.
(33) Gao, Y.; Ogilby, P. R. *Macromolecules* **1992**, *25* (19), 4962.
(34) Masoumi, Z.; Stoeva, V.; Yekta, A.; Pang, Z.; Manners, I.; Winnik, M. A. *Chem. Phys. Lett.* **1996**, *261*, 551.
(35) Pang, Z.; Gu, X.; Yekta, A.; Masoumi, Z.; Coll, J. B.; Winnik, M. A.; Manners, I. *Adv. Mater.* **1996**, *8* (9), 768.
(36) Jayarajah, C. N.; Yekta, A.; Manners, I.; Winnik, M. A. *Macromolecules* **2000**, *33* (15), 5693.
(37) Lu, X.; Manners, I.; Winnik, M. A. In *Fluorescence Spectroscopy: New Trends in Fluorescence Spectroscopy*; Valeur, B., Brochon, J. C., Eds.; Springer-Verlag: New York, 2001, Ch. 12, p 229.
(38) Ruffolo, R.; Evans, C.; Liu, X. H.; Ni, Y.; Pang, Z.; Park, P.; McWilliams, A.; Gu, X.; Lu, X.; Yekta, A.; Winnik, M. A.; Manners, I. *Anal. Chem.* **2000**, *72*, 1894.
(39) Mills, A.; Chang, Q. *Analyst* **1992**, *117*, 1461.
(40) Wolfbeis, O. S.; Leiner, M. J. P.; Posch, H. E. *Mikrochim. Acta* **1986**, *III*, 359.
(41) Moreno-Bondi, M. C.; Wolfbeis, O. S.; Leiner, M. J. P.; Schaffar, B. P. H. *Anal. Chem.* **1990**, *62*, 2377−2380.
(42) Lippitsch, M. E.; Pusterhofer, J.; Leiner, M. J. P.; Wolfbeis, O. S. *Anal. Chim. Acta* **1988**, *205*, 1−6.
(43) Hartmann, P.; Leiner, M. J. P.; Lippitsch, M. E. *Sens. Actuators B* **1995**, *29*, 251.
(44) Meier, B.; Werner, T.; Klimant, I.; Wolfbeis, O. S. *Sens. Actuators B* **1995**, *29*, 240−245.
(45) Sacksteder, L.; Demas, J. N.; DeGraff, B. A. *Anal. Chem.* **1993**, *65*, 3480.
(46) Carraway, E. R.; Demas, J. N.; DeGraff, B. A.; Bacon, J. R. *Anal. Chem.* **1991**, *63*, 337.
(47) Carraway, E. R.; Demas, J. N.; DeGraff, B. A. *Langmuir* **1991**, *7*, 2991.
(48) Xu, W.; McDonough, R. C.; Langsdorf, B.; Demas, J. N.; DeGraff, B. A. *Anal. Chem.* **1994**, *66*, 4133.
(49) Guillet, J. *Polymer Photophysics and Photochemistry: Introduction to the Study of Photoprocesses in Macromolecules*; Cambridge University Press: New York, 1985.
(50) Masoumi, Z.; Stoeva, V.; Yekta, A.; Winnik, M. A.; Manners, I. In *Polymers and Organic Solids*; Shi, L., Zhu, D., Eds.; Science Press: Beijing, 1997; p 157.

(51) Liang, M.; Manners, I. *J. Am. Chem. Soc.* **1991**, *113*, 4044.
(52) Ni, Y.; Stammer, A.; Liang, M.; Massey, J.; Vancso, G. J.; Manners, I. *Macromolecules* **1992**, *25*, 7119.
(53) Ni, Y.; Park, P.; Liang, M.; Massey, J.; Waddling, C.; Manners, I. *Macromolecules* **1996**, *29*, 3401.
(54) Lu, X.; Manners, I.; Winnik, M. A. *Macromolecules* **2001**, *34*, 1917.
(55) Gouin, S.; Gouterman, M. *J. Appl. Polym. Sci.* **2000**, *77*, 2824.
(56) One should also note that, as the intensity of the emitted light is decreased, a large background signal due to scattered light might make it difficult to detect subtle changes of intensity due to an oxygen pressure change.
(57) Ponomarev, S.; Gouterman, M. Presented at the 6th Annual Pressure Sensitive Paint Workshop, Seattle, WA, Oct 6−8, 1998.
(58) Scroggin, A.; Slamovich, E.; Lachendro, N.; Sakaue, H.; Sullivan, J.; Asai, K. Presented at the 7th Annual Pressure Sensitive Paint Workshop, West Lafayette, IN, Oct 11−13, 1999.
(59) *Hybrid Organic−Inorganic Composites*; Mark, J. E., Lee, Y., Bianconi, P. A., Eds.; American Chemical Society: Washington, D.C., 1995.
(60) Ahmad, Z.; Mark, J. E. *Mater. Sci. Eng. C−Biomimetics* **1998**, *6*, 183.
(61) Mark, J. E.; Schaeffer, D. W. In *Polymer Blend Based Composites*; Mark, J. E., Schaeffer, D. W., Eds.; Materials Research Society: Pittsburgh, PA, 1990; p 51.
(62) Panusa, A.; Flamini, A.; Poli, N. *Chem. Mater.* **1996**, *8*, 1202.
(63) de Mello, A. J.; Crystall, B.; Rumbles, G. *J. Colloid Interface Sci.* **1995**, *169*, 161.
(64) Wehry, E. L. Effects of Molecular Environment on Fluorescence and Phosphorescence. In *Practical Fluorescence*; Guilbault, G. G., Ed.; Marcel Dekker: New York, 1990; pp 154−157.
(65) Lam, S. K.; Lo, D. *Chem. Phys. Lett.* **1997**, *281*, 35.
(66) Xavier, M. P.; Garcia-Fresnadillo, D.; Moreno-Bondi, M. C.; Orellana, G. *Anal. Chem.* **1998**, *70*, 5184.
(67) Mingoarranz, F. J.; Moreno-Bondi, M. C.; Garcia-Fresnadillo, D.; de Dios, C.; Orellana, G. *Mikrochim. Acta* **1995**, *121*, 107.
(68) Barrer, R. M. In *Diffusion in Polymers*; Crank, J., Park, G. S., Eds.; Academic Press: New York, 1968; pp 164−217.
(69) Paul, D. R.; Kemp, D. R. *J. Polym. Sci.: Symp.* **1973**, *41*, 79.
(70) Van Amerongen, G. J. *Rubber Chem. Technol.* **1964**, *37*, 1067.
(71) Litvinov, V. M.; Spiess, H. W. *Makromol. Chem.* **1991**, *192*, 3005; **1992**, *193*, 1184.
(72) Kirst, K. U.; Kremer, F.; Litvinov, V. M. *Macromolecules* **1993**, *26*, 975.
(73) Tsagaropoulos, G.; Eisenberg, A. *Macromolecules* **1995**, *28*, 396; **1995**, *28*, 6067.
(74) Long, D.; Lequeux, F. *Eur. Phys. J. E.* **2001**, *4*, 371.
(75) Turro, N. J. *Modern Molecular Photochemistry*; Benjamin-Cummings: Menlo Park, CA, 1978.
(76) Pauly, S. In *Polymer Handbook*, 3rd ed.; Brandrup, J., Immergut, E. H., Eds.; Wiley-Interscience: New York, 1989; pp VI435−VI449.
(77) Naylor, T. In *Comprehensive Polymer Science*; Allen, G., Bevington, J. C., Eds.; Pergamon Press: Oxford, U.K., 1989; Vol. 2, pp 643−668.
(78) (a) Koros, W. J.; Hellums, M. W. In *Encyclopedia of Polymer Science and Engineering, Supplement*; Mark, H. F., Overberger, C. G., Bikales, N. M., Menges, G., Kroschwitz, J. I., Eds.; Wiley: New York, 1985. (b) Poulsen, L.; Ogilby, P. R. *J. Phys. Chem. A* **2000**, *104*, 2573.
(79) Kamiya, Y.; Naito, Y.; Hirose, T.; Mizoguchi, K. *J. Polym. Sci. B: Polym. Phys.* **1990**, *28*, 1297.
(80) Joly, C.; Goizet, S.; Schrotter, J. C.; Sanchez, J.; Escoubes, M. *J. Membr. Sci.* **1997**, *130*, 63.
(81) Joly, C.; Smaihi, M.; Porcar, L.; Noble, R. D. *Chem. Mater.* **1999**, *11*, 2331.
(82) (a) Hartmann, P.; Leiner, M. J. P.; Lippitsch, M. E. *Anal. Chem.* **1995**, *67*, 88. (b) Draxler, S.; Lippitsch, M. E.; Klimant, I.; Kraus, H.; Wolfbeis, O. S. *J. Phys. Chem.* **1995**, *99*, 3162. (c) Draxler, S.; Lippitsch, M. E. *Anal. Chem.* **1996**, *68*, 753.
(83) Lakowicz, J. R. *Principles of Fluorescence Spectroscopy*; Kluwer Academic/Plenum Publishers: New York, 1999; pp 367−394.
(84) Adamson, A. W. *Physical Chemsitry of Surfaces*; John Wiley & Sons: New York, 1982; pp 421−426.
(85) Krasnansky, R.; Koike, K.; Thomas, J. K. *J. Phys. Chem.* **1990**, *94*, 4521.
(86) Sakaue, H.; Sullivan, J. P.; Asai, K. Presented at the 7th Annual Pressure Sensitive Paint Workshop, West Lafayette, IN, Oct 11−13, 1999.
(87) Demas, J. N.; DeGraff, B. A.; Xu, W. *Anal. Chem.* **1995**, *67*, 1377.
(88) Rideal, E. K. *Cambridge Philos. Soc.* **1939**, *35*, 130.
(89) Hinshelwood, C. W. *Kinetics of Chemical Change*; Clarendon: Oxford, U.K., 1940.
(90) Thomas, J. K. *Chem. Rev.* **1993**, *93*, 301.
(91) Rutten, S. A.; Thomas, J. K. *J. Phys. Chem. B* **1999**, *103*, 1278.
(92) Wang, H.; Harris, J. M. *J. Phys. Chem.* **1995**, *99*, 16999.
(93) Freeman, D. L.; Doll, J. D. *J. Chem. Phys.* **1983**, *78*, 6002.
(94) Freeman, D. L.; Doll, J. D. *J. Chem. Phys.* **1983**, *79*, 2343.
(95) Drake, J. M.; Levitz, P.; Turro, N. J.; Nitsche, K. S.; Cassidy, K. F. *J. Phys. Chem.* **1988**, *92*, 4680.
(96) Levin, P. P.; Costa, S. M. B.; Ferreira, L. F. V.; Lopes, J. M.; Ribeiro, F. R. *J. Phys. Chem. B* **1997**, *101*, 1355.
(97) Springob, C.; Wolff, T. *J. Photochem. Photobiol. A: Chem.* **1996**, *101*, 75.
(98) Krasnansky, R.; Thomas, J. K. *J. Photochem. Photobiol. A: Chem.* **1991**, *57*, 81.
(99) Pankasem, S.; Thomas, J. K. *J. Phys. Chem.* **1991**, *95*, 7385.
(100) Krasnansky, R.; Thomas, J. K. *Colloid Chem. Silica* **1994**, *234*, 223.
(101) Samuel, J.; Ottolenghi, M.; Avnir, D. *J. Phys. Chem.* **1992**, *96*, 6398.
(102) Katz, O.; Samuael, J.; Avnir, D.; Ottolengthi, M. *J. Phys. Chem.* **1995**, *99*, 14893.
(103) Wolfgang, S.; Gafney, H. D. *J. Phys. Chem.* **1983**, *87*, 5395.
(104) Wong, A. L.; Hunnicutt, M. L.; Harris, J. M. *J. Phys. Chem.* **1991**, *95*, 4489.
(105) Wong, A. L.; Harris, J. M. *J. Phys. Chem.* **1991**, *95*, 5895.
(106) He, H.; Fraatz, R. J.; Leiner, M. J. P.; Rehn, M. M.; Tusa, J. K. *Sens. Actuators B* **1995**, *29*, 246.

CM011029K